BIOCHEMISTRY
including biophysical chemistry & molecular biology

Article

pubs.acs.org/biochemistry

Enzyme-Dependent Lysine Deprotonation in EZH2 Catalysis

D. Randal Kipp, Christopher M. Quinn, and Pascal D. Fortin*

Novartis Institutes for Biomedical Research, 250 Massachusetts Avenue, Cambridge, Massachusetts 02139, United States

Supporting Information

ABSTRACT: Protein lysine methyltransferases (PKMTs) are key players in epigenetic regulation and have been associated with a variety of diseases, including cancers. The catalytic subunit of Polycomb Repressive Complex 2, EZH2 (EC 2.1.1.43), is a PKMT and a member of a family of SET domain lysine methyltransferases that catalyze the transfer of a methyl group from *S*-adenosyl-L-methionine to lysine 27 of histone 3 (H3K27). Wild-type (WT) EZH2 primarily catalyzes the mono- and dimethylation of H3K27; however, a clinically relevant active site mutation (Y641F) has been shown to alter the reaction specificity, dominantly catalyzing trimethylation of H3K27, and has been linked to tumor genesis and maintenance. Herein, we explore the chemical mechanism of methyl transfer by EZH2 and its Y641F mutant with pH−rate profiles and solvent kinetic isotope effects (sKIEs) using a short peptide derived from histone H3 [H3(21−44)]. A key component of the chemical reaction is the essential deprotonation of the ϵ-NH_3^+ group of lysine to accommodate subsequent methylation. This deprotonation has been suggested by independent studies (1) to occur prior to binding to the enzyme (by bulk solvent) or (2) to be facilitated within the active site following binding, either (a) by the enzyme itself or (b) by a water molecule with access to the binding pocket. Our pH−rate and sKIE data best support a model in which lysine deprotonation is enzyme-dependent and at least partially rate-limiting. Furthermore, our experimental data are in agreement with prior computational models involving enzyme-dependent solvent deprotonation through a channel providing bulk solvent access to the active site. The mechanism of deprotonation and the rate-limiting catalytic steps appear to be unchanged between the WT and Y641F mutant enzymes, despite their activities being highly dependent on different substrate methylation states, suggesting determinants of substrate and product specificity in EZH2 are independent of catalytic events limiting the steady-state rate.

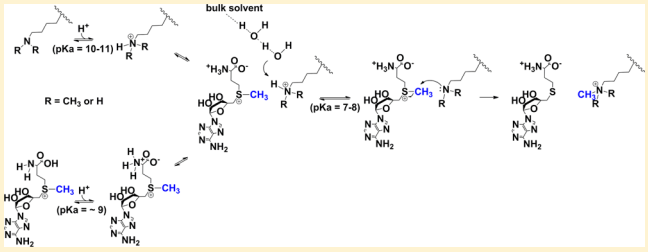

Accessibility of genomic DNA to the gene expression pipeline is under tight epigenetic control, largely through the structural fine-tuning of heterochromatin. Combinatorial epigenetic protein−protein interactions, protein−DNA interactions, and site-specific covalent protein and DNA modifications (such as methylation, acetylation, phosphorylation, etc.) regulate gene expression patterns and are therefore critical for normal cell processes.[1] Aberrant activity of epigenetic gene products has been associated with a variety of diseases resulting from either hyperactivation of disease-promoting gene products (such as oncoproteins) or silencing of disease-reducing gene products (such as tumor suppressors).[2,3] Therefore, targeting epigenetic modulators is a promising strategy for the development of cancer therapeutics.

A key epigenetic modification involved in gene activation and silencing is protein methylation.[4] Methylation of core histone subunits, which comprise the nucleosome around which the DNA is wound for packaging, is facilitated by a variety of protein methyltransferases that methylate specific side-chain amines of the histone lysine or arginine residues.[4,5] The catalytic subunit of Polycomb Repressive Complex 2 (PRC2), EZH2 (EC 2.1.1.43), is a protein lysine methyltransferase (PKMT) responsible for the mono- and dimethylation of lysine 27 of histone 3 (H3K27) with a marginal activity for H3K27 trimethylation.[6] A mutation of a tyrosine residue (Y641) within the lysine binding site effectively reverses the substrate specificity of the enzyme, abrogating its ability to produce mono- and dimethylation products while allowing EZH2 to predominantly produce trimethylated H3K27 (Scheme 1).[6,7] Thus, the overall consequence of the Y641F mutation is both loss of function (reduced levels of mono- and dimethylation) and gain of function (increased level of trimethylation). Importantly, the EZH2 Y641F mutation is heterozygous, with cancer cells containing one mutant allele while maintaining the second wild-type (WT) allele. This suggests that mutant EZH2 and WT EZH2 work in concert to hypermethylate H3K27 and facilitate excessive gene silencing.[8] Notably, approximately 20% of patients with germinal center B cell (GCB)-derived diffuse large B cell lymphoma (DLBCL), the most frequent lymphoma (accounting for an estimated 35% of lymphoma worldwide), carry activating mutations of EZH2.[9] Aberrant EZH2 activity is also observed in other diseases such as follicular lymphomas, prostate cancers, rhabdoid tumors, parathyroid adenomas, and melanomas; the disruption of PRC2/EZH2 activity has been shown to reduce the rate of cancer cell growth in a number of

Received: June 21, 2013
Revised: August 7, 2013
Published: September 3, 2013

dx.doi.org/10.1021/bi400805w | *Biochemistry* 2013, 52, 6866−6878

Scheme 1. Methyltransferase Reactions Catalyzed by EZH2

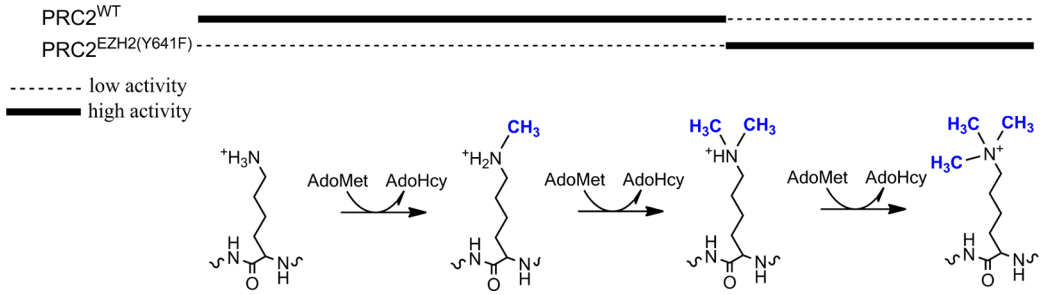

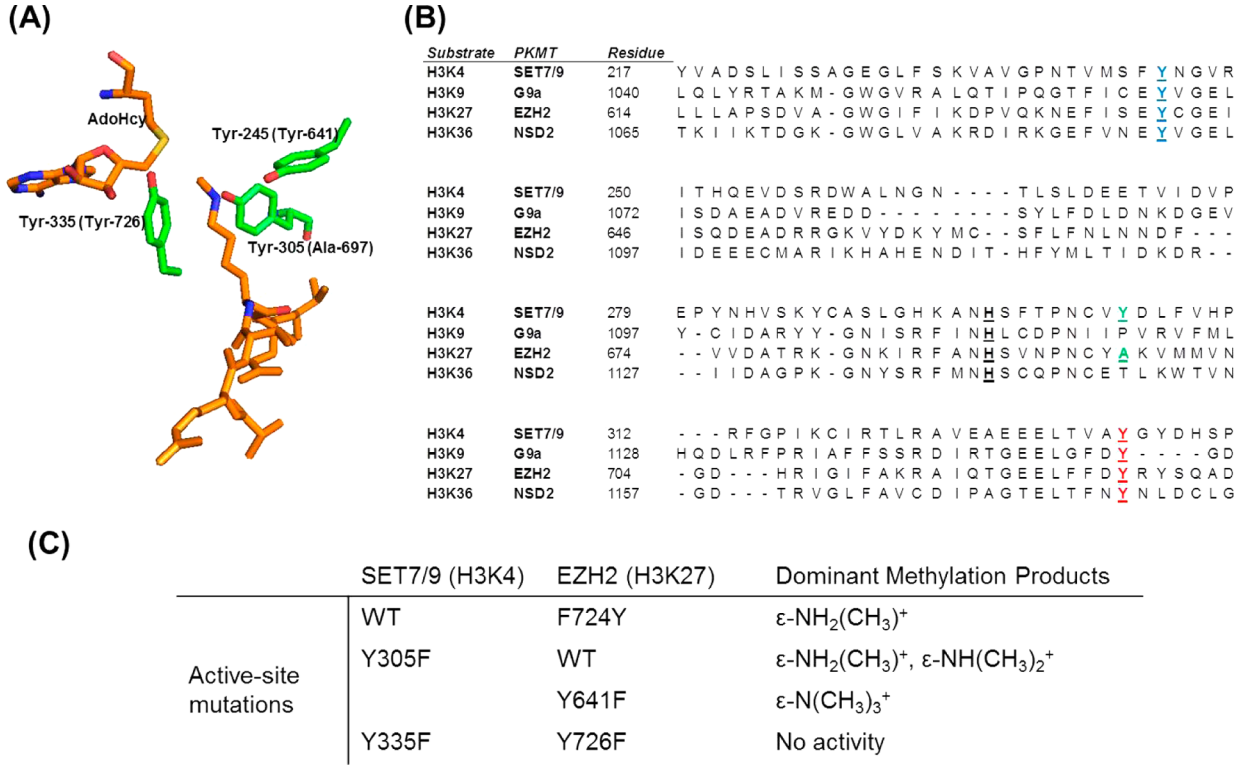

(C)

	SET7/9 (H3K4)	EZH2 (H3K27)	Dominant Methylation Products
Active-site mutations	WT	F724Y	ε-$NH_2(CH_3)^+$
	Y305F	WT	ε-$NH_2(CH_3)^+$, ε-$NH(CH_3)_2^+$
		Y641F	ε-$N(CH_3)_3^+$
	Y335F	Y726F	No activity

Figure 1. Active site tyrosine residues correlate with methylation activity and specificity. (A) ε-$NH_2(CH_3)^+$-lysine and AdoHcy in the active site of SET7/9. Structural information was obtained from Protein Data Bank entry 1O9S.[24] Residue numbers are shown for SET7/9, and the corresponding residues in EZH2 are given in parentheses. (B) Sequence comparisons of SET domain protein lysine methyltransferases. SET domains of representative PKMTs from each histone 3 methylation site. The absolutely conserved tyrosine required for enzymatic activity (Y726 in EZH2) is colored red in the bottom row. The mutated tyrosine in these studies (Y641F) is colored blue in the top row. The essential histidine and Tyr-305 of SET7/9 (which when mutated changes activity from mono- to dimethylation) is colored green. (C) Active site tyrosine mutations in SET7/9, corresponding mutations in EZH2, and the resulting dominant methylation product from each mutation.

cancer models, and ongoing trials are examining the clinical efficacy of EZH2 inhibitors.[9−14]

EZH2 catalyzes methyl group transfer from an *S*-adenosyl-L-methionine (AdoMet) donor to the ε-amino group of its side-chain lysine acceptor (Scheme 1), generating methylated H3K27 and *S*-adenosyl-L-homocysteine (AdoHcy).[15] Although no high-resolution structural information is available to date for EZH2, sequence comparisons suggest it belongs to a family of PKMTs with a structural domain, the SET domain, featuring independent AdoMet and lysine binding sites bisected by a pseudoknot that provides a tunnel for methyl transfer.[16−18] Among the SET domain PKMTs characterized, a theme has emerged in that the ability to form mono-, di-, or trimethylated products correlates with the presence or absence of tyrosine residues in specific locations in the lysine binding site[16−22] (although this effect is not limited to tyrosine[23]) (Figure 1). For example, the PKMT SET7/9 contains two key tyrosine residues, Y245 and Y305, which correlate with the WT monomethyltransferase activity of SET7/9.[24] A sequence alignment of SET7/9 with EZH2 shows an alanine in the position analogous to the Y305 residue of SET7/9 (Figure 1B). Indeed, both WT EZH2 and SET7/9 Y305F have been shown to give dimethylated products.[25] Furthermore, the Y641F mutation in EZH2 that is associated with cancer phenotypes and an increased level of trimethylated product is analogous to Y245 of SET7/9 (Figure 1A,B), suggesting tightly regulated product specificity by tyrosine residues in the lysine binding site of SET domain PKMTs.

The mechanistic basis for changes in product specificity resulting from specific mutations has been explored through crystallographic and computational approaches for a variety of SET domain PKMTs; however, no reports have yet addressed

dx.doi.org/10.1021/bi400805w | *Biochemistry* 2013, 52, 6866−6878

the influence of these mutations on the kinetic and chemical mechanism of EZH2. Furthermore, few experimental data have been reported on the kinetic and chemical mechanism of SET domain PKMTs in general. While it is widely assumed that the methyl transfer reaction proceeds through an S_N2 mechanism, additional features of the chemical mechanism, specifically the required deprotonation of the Lys-ε-NH_3^+ to accommodate the incoming methyl group, have been largely unexplored experimentally. A variety of crystallographic studies led to early speculation that an absolutely essential active site tyrosine acts as a general base in deprotonating lysine,[26−28] a model given additional support by molecular dynamics (MD) and hybrid quantum mechanics/molecular mechanics (QM/MM) simulations of SET7/9.[29] However, subsequent crystallographic studies of the PKMT Rubisco suggested that the essential tyrosine was incapable of deprotonating lysine, instead suggesting bulk solvent deprotonation and preferential binding to the Lys-ε-NH_2.[30] Conversely, a series of QM/MM and MD studies of multiple PKMTs were used to generate a model in which a water channel induced by formation of the Lys-ε-NH_3^+·AdoMet·Enz ternary complex provides active site access to bulk solvent, permitting enzyme-dependent solvent deprotonation,[31−36] and subsequent crystallographic and mutagenesis studies have provided evidence that water molecules participate in the active site ensemble.[37,38]

Herein, we explore the mechanism of lysine deprotonation by EZH2 and its loss-of-function/gain-of-function mutant (Y641F) in mono-, di-, and trimethylation with pH−rate profiles, solvent deuterium kinetic isotope effects, and proton inventories. Our aims are to understand the role of EZH2 in deprotonating its lysine substrate, to explore the effects of the substrate and product specificity-altering Y641F mutation on the enzymatic mechanism, and to provide an experimental evaluation of previous models stemming from crystallographic or computational analyses.

EXPERIMENTAL PROCEDURES

Materials. $PRC2^{WT}$ [five-member complex (EZH2, SUZ12, EED, AEBP2, and RbAp48)] was a gift from the Center for Proteomic Chemistry of the Novartis Institutes for Biomedical Research, and $PRC2^{EZH2(Y641F)}$ (five-member complex) was obtained through Viva Biotech Ltd. (Shanghai, China) (prepared according to an established protocol[39]). H3K27 peptide substrates [H_2N-ATKAARKSAPATGGVKKPHRYRP-GG(K-Biotin)-OH] were purchased with unmethylated (H3[21−44]), monomethylated {H3[21−44(K27-CH_3)]}, and dimethylated (H3{21−44[K27-$(CH_3)_2$]}) lysine 27 from New England Peptide (Gardner, MA). [$\beta,\beta,\gamma,\gamma$-$^2H_4$]AdoHcy was purchased from Cayman Chemical Co. (Ann Arbor, MI). [$^2H_2$]H_2O was purchased from Cambridge Isotope Laboratories, Inc. (Andover, MA). General lab supplies and reagents were purchased through VWR International, LLC (Radnor, PA).

AdoHcy Detection (methyltransferase assay). EZH2 methyltransferase activity was measured with a discontinuous assay monitoring AdoHcy product formation detected by liquid chromatography and tandem mass spectrometry (LC−MS/MS). Assays were performed in a 384-well plate format in 10 μL reaction volumes. Reactions were quenched with 5 μL of 0.3% HCOOH and mixtures supplemented with 5 μL of 0.8 μM [$\beta,\beta,\gamma,\gamma$-$^2H_4$]AdoHcy (final concentration of 0.2 μM) in 20% dimethyl sulfoxide (DMSO) as an internal standard. Quenched reaction mixtures were then sonicated for 3 min using a Hendrix SM-100 sonicator (Microsonics Systems) and centrifuged at 1000 rpm for 60 s. Samples were analyzed using a 4000 QTRAP Hybrid Triple Quadrupole/Linear Ion trap LC−MS/MS system (AB Sciex). Ten microliters of each sample was loaded onto polar end-capped C18 reversed phase columns (Synergi Hydro-RP, 2.5 μm, 100 Å, 20 mm × 2 mm, Phenomenex) equilibrated with 0.1% HCOOH in H_2O (mobile phase A). Reaction components were separated from AdoHcy with the following step gradient using 0.1% HCOOH in acetonitrile (CH_3CN) (mobile phase B) at a flow rate of 0.5 mL/min: (1) 100% mobile phase A for 12 s, (2) 50% mobile phase A and 50% mobile phase B for 36 s, (3) 5% mobile phase A and 95% mobile phase B for 12 s, and (4) 100% mobile phase A for 60 s. MS/MS data were acquired during an 18 s window starting at 30 s following sample loading utilizing multiple-reaction monitoring in positive ion mode to detect parent/daughter ion combinations with mass-to-charge ratios of 385/136 Da for AdoHcy and 389/136 Da for [$\beta,\beta,\gamma,\gamma$-$^2H_4$]AdoHcy.

Methylation Reaction Specificity. Relative activities of each methylation reaction were measured using the AdoHcy detection LC−MS/MS assay. Reactions were performed at a fixed saturating concentration of AdoMet (10 μM) with varied H3[21−44] peptides at room temperature in 20 mM Tris (pH 7.5), 0.5 mM dithiothreitol (DTT), and 0.01% Triton X-100. For the $PRC2^{WT}$ reactions, concentrations of H3[21−44] and H3[21−44(K27-CH_3)] ranged from 150 nM to 10 μM and those of H3{21−44[K27-$(CH_3)_2$]} from 150 nM to 100 μM. For the $PRC2^{EZH2(Y641F)}$ reactions, concentrations of H3[21−44] and H3[21−44(K27-CH_3)] ranged from 150 nM to 100 μM and concentrations of H3{21−44[K27-$(CH_3)_2$]} from 150 nM to 10 μM. Reactions at each substrate concentration were conducted with three discontinuous time points (30, 60, and 90 min) in triplicate, and initial rates (v_i) were obtained from linear regression of AdoHcy concentration versus time. Steady-state parameters were obtained by plotting v_i as a function of H3[21−44] concentration and fitting to eq 1

$$v_i = \frac{^{app}k_{cat}[E_t][S]}{^{app}K_m + [S]} \quad (1)$$

where $^{app}k_{cat}$ is the apparent first-order rate constant (turnover rate constant at a saturating H3[21−44] concentration) obtained from varying H3[21−44] concentrations at a constant AdoMet concentration of 10 μM and $^{app}K_m$ is the apparent K_m for the H3[21−44] peptide substrate under the same conditions.

pH−Rate Profiles. To obtain pH−rate parameters on k_{cat} for each methylation reaction, full bisubstrate saturation kinetics were performed at pH 7.0−9.0 at 0.5 unit increments. To test for ionic strength sensitivity from the buffer conditions at varying pH [the ionic strength of 20 mM Tris increases from 2 to 19 mM from pH 9.0 to 7.0 because of an increase in the number of Cl^- ions in the conjugate acid form of Tris (Tris-HCl)], initial rates were measured at room temperature in 20 mM Tris (pH 8.1), 0.5 mM DTT, 0.01% Triton X-100, and 0−20 mM NaCl (5 mM increments) at saturating concentrations of both substrates (for effects on the first-order rate constant, k_{cat}) and limiting concentrations of each substrate at saturating concentrations of the other (for effects on the second-order rate constants, k_{cat}/K_{AdoMet} and $k_{cat}/K_{H3[21-44]}$). Because of the significant ionic strength effect on all parameters (Figure S1A−C of the Supporting Information), 1.0 M NaCl was added to

the buffer at each pH to give a total ionic strength of 19 mM in each reaction mixture.

To evaluate the pH stability of the enzyme, 350 nM $PRC2^{WT}$ was incubated in a mixed 20 mM Tris-Glycine-CAPS buffer between pH 7.0 and 11.5 at 0.5 unit increments for 5 min, followed by dilution to 2.5 nM in 20 mM Tris (pH 8.1) (known active pH), 0.5 mM DTT, and 0.01% Triton X-100, and reacted with 2 μM AdoMet and 0.5 μM H3[21−44]. Reactions were conducted in triplicate and quenched at 10, 30, and 60 min to obtain initial rates. The activity of PRC2 begins to be lost irreversibly at pH >9.0 (Figure S1D of the Supporting Information).

pH−rate profile measurements were taken over five concentrations of H3[21−44] peptides (between 20 nM and 10 μM) at five fixed AdoMet concentrations (between 20 nM and 10 μM) in 20 mM Tris (pH 7.0−9.0, 0.5 unit increments, ionic strength of 19 mM), 0.5 mM DTT, and 0.01% Triton X-100. Reactions were initiated with 2.5 nM $PRC2^{WT}$ (for mono- and dimethylation) and 2.5 nM $PRC2^{EZH2(Y641F)}$ (for trimethylation) and at each concentration were quenched at three time points (between 20 and 90 min) in triplicate to obtain v_i. Steady-state parameters were obtained at each pH unit by plotting v_i as a function of substrate 1 concentration at each substrate 2 concentration and fitting globally to eq 2 for a random bi-bi sequential mechanism[40]

$$v_i = \frac{k_{cat}[E_t][A][B]}{\alpha K_{ia}K_b + \alpha K_b[A] + \alpha K_a[B] + [A][B]} \quad (2)$$

where [A] and [B] are the substrate concentrations, k_{cat} is the first-order rate constant describing the turnover rate at full saturation of both substrates, and $[E_t]$ is the total enzyme concentration (K_{ia}, K_a, and K_b represent the apparent inhibition constant of substrate A, the apparent K_m of substrate A, and the apparent K_m of substrate B, respectively).

As data in the low-substrate region are often limited in the saturation profiles, pH−rate parameters for k_{cat}/K_{AdoMet} and $k_{cat}/K_{H3[21-44]}$ were obtained in independent experiments with increasing concentrations of substrate in a range below their respective K_m values (50−300 nM) with the concentration of the other substrate being 10 μM. Reactions were initiated with 2.5 nM $PRC2^{WT}$ (for mono- and dimethylation) and 2.5 nM $PRC2^{EZH2(Y641F)}$ (for trimethylation) and quenched at 90, 120, 150, and 180 min in triplicate. k_{cat}/K_{AdoMet} and $k_{cat}/K_{H3[21-44]}$ values were obtained for each substrate from linear regression of v_i versus [substrate]. Similar reactions were performed with both substrates at 10 μM, and sufficient saturation was confirmed by comparing the resulting pH−rate profiles to those generated from the bisubtrate saturation profiles (Figure S8 of the Supporting Information).

To analyze pH−rate profiles, the log values of each rate constant (k_{cat}, k_{cat}/K_{AdoMet}, and $k_{cat}/K_{H3[21-44]}$) were plotted as a function of pH. Plots in which the rate increased with pH with a plateau in the basic region of the curve were fit to eq 3, and plots in which the pH−rate dependency was bell-shaped were fit to eq 4

$$\log(y) = \log\left(\frac{c}{1 + \frac{H}{K}}\right) \quad (3)$$

$$\log(y) = \log\left(\frac{c}{1 + \frac{H}{K_1} + \frac{K_2}{H}}\right) \quad (4)$$

where y is the measured rate constant, c is the maximal value of y, H is the hydrogen ion concentration, and K values are acid dissociation constants, where $pK_a = -\log(K)$.

Solvent Kinetic Isotope Effects (sKIEs). sKIE measurements were taken over five concentrations of H3[21−44] peptides, at five fixed AdoMet concentrations (both ranging from 20 nM to 10 μM). Reactions were performed in H_2O [20 mM Tris (pH 9.0, ionic strength of 6 mM), 0.5 mM DTT, and 0.01% Triton X-100] and 90% D_2O {20 mM Tris [pH(D) 9.0, ionic strength of 6 mM], 0.5 mM DTT, and 0.01% Triton X-100}. Additionally, a viscosity control was performed for each reaction under the same condition as with H_2O with 9% glycerol to mimic the viscosity effect of D_2O. Twenty millimolar Tris (pD 9.0) in 99.8% D_2O was initially prepared in accordance with an increase in the pK_a of Tris to 8.56 in D_2O.[41] Consequently, more conjugate acid (Tris-HCl) was used to reach the desired pH, slightly increasing the ionic strength (which was corrected for in the H_2O reaction by supplementing with 1.0 M NaCl). Reactions were initiated with 2.5 nM $PRC2^{WT}$ (for mono- and dimethylation) and 2.5 nM $PRC2^{EZH2(Y641F)}$ (for trimethylation) and at each concentration were quenched at 30, 60, and 90 min in triplicate to obtain v_i. k_{cat} values were obtained from fitting the full bisubtrate profile globally to eq 2. sKIE values were calculated as the ratio of reaction rates in H_2O to those in 90% D_2O.

There is a significant reduction in $K_{H3[21-44]}$ at pH 9.0 in the absence of a high salt concentration (the conditions of the solvent KIEs) (Table S1 of the Supporting Information). Coupled with the inherent difficulty of obtaining initial rates at saturating AdoMet concentrations because of the presence of trace amounts of AdoHcy in stock solutions of AdoMet (limiting accurate LC−MS quantitation), $k_{cat}/K_{H3[21-44]}$ parameters could not be measured as they were in the pH−rate studies. Therefore, sKIEs for $k_{cat}/K_{H3[21-44]}$ were obtained from the steady-state parameters obtained from fitting the bisubstrate saturation profiles to eq 2. k_{cat}/K_{AdoMet} profiles were determined at pH(D) 8.0 (near pH-independent value obtained from the pH−rate profiles) with increasing concentrations of AdoMet in a range below K_{AdoMet} (50−300 nM) at 10 μM H3[21−44] for each $PRC2^{WT}$ mono- and dimethylation and $PRC2^{EZH2(Y641F)}$ trimethylation by reacting with 2.5 nM enzyme and quenching at 90, 120, 150, and 180 min to obtain v_i. k_{cat}/K_{AdoMet} values were determined by linear regression of v_i versus H3[21−44] concentration.

Proton Inventories. Proton inventory analysis was conducted by reacting 10 μM AdoMet and 10 μM H3[21−44] with 2.5 nM enzyme in 0−90% D_2O (10% increments) in 20 mM Tris [pH(D) 9.0], 0.5 mM DTT, and 0.01% Triton X-100; 1.0 M NaCl was added to the buffer at each percent D_2O increment to keep the ionic strength constant at 6 mM. Reactions were performed in triplicate and quenched at 10, 20, 30, 40, and 50 min. Initial rates were obtained from linear regression of the AdoHcy concentration (nanomolar) versus time. Ratios of the rates obtained at each increment of D_2O (v_n) versus the rates in H_2O (v_H) were plotted against the D/H ratio, and transition-state fractionation factors were obtained by fitting the data to eq 5

dx.doi.org/10.1021/bi400805w | Biochemistry 2013, 52, 6866−6878

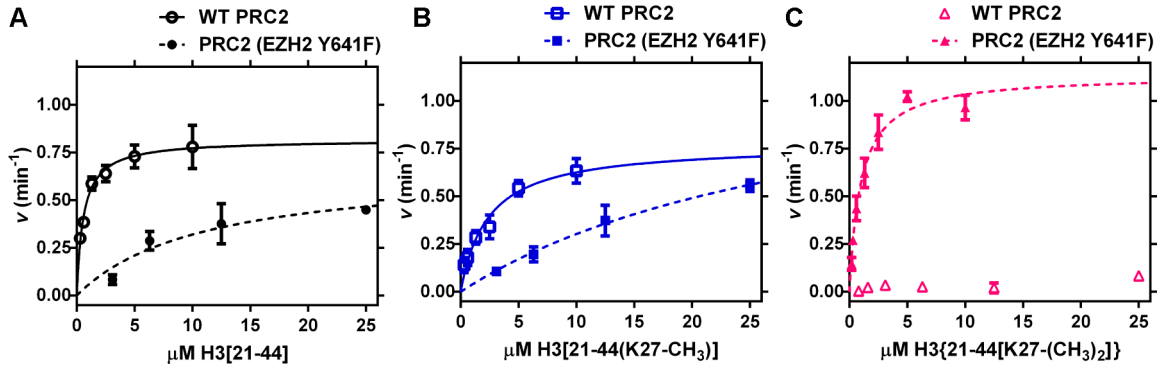

Figure 2. Kinetics of mono-, di-, and trimethylation by $PRC2^{WT}$ and $PRC2^{EZH2(Y641F)}$. (A) Monomethylation by $PRC2^{WT}$ (○) and $PRC2^{EZH2(Y641F)}$ (●), (B) dimethylation by $PRC2^{WT}$ (□) and $PRC2^{EZH2(Y641F)}$ (■), and (C) trimethylation by $PRC2^{WT}$ (△) and $PRC2^{EZH2(Y641F)}$ (▲) in the presence of 10 μM AdoMet in 20 mM Tris (pH 7.5), 0.5 mM DTT, and 0.01% Triton X-100. Initial rates are plotted against multiple concentrations of H3 peptide and the data fit to eq 1. Significant effects on $K_{H3[21-44]}$ resulting from the EZH2 Y641F mutation in mono- and dimethylation and the complete loss of activity under these assay conditions for trimethylation by the WT enzyme are illustrated (see Table 1 for the catalytic parameters).

Table 1. Catalytic Parameters of Mono-, Di-, and Trimethylation by $PRC2^{WT}$ and $PRC2^{EZH2(Y641F)}$ at a Saturating AdoMet Concentration

enzyme	H3 peptide	$^{app}k_{cat}$ ($\times10^{-2}$ s^{-1})	$^{app}K_{H3[21-44]}$ ($\times10^{-6}$ M)	$^{app}k_{cat}/K_{H3[21-44]}$ ($\times10^{4}$ M^{-1} s^{-1})
$PRC2^{WT}$	21–44	1.37 ± 0.05	0.6 ± 0.1	2.28 ± 0.39
	21–44[K27-CH_3]	1.28 ± 0.10	2.4 ± 0.5	0.53 ± 0.14
	21–44[K27-$(CH_3)_2$]	no activity	–	–
$PRC2^{EZH2(Y641F)}$	21–44	1.12 ± 0.21	11.0 ± 4.7	0.10 ± 0.05
	21–44[K27-CH_3]	2.17 ± 0.50	33.0 ± 11.8	0.07 ± 0.03
	21–44[K27-$(CH_3)_2$]	1.90 ± 0.07	1.0 ± 0.1	1.90 ± 0.20

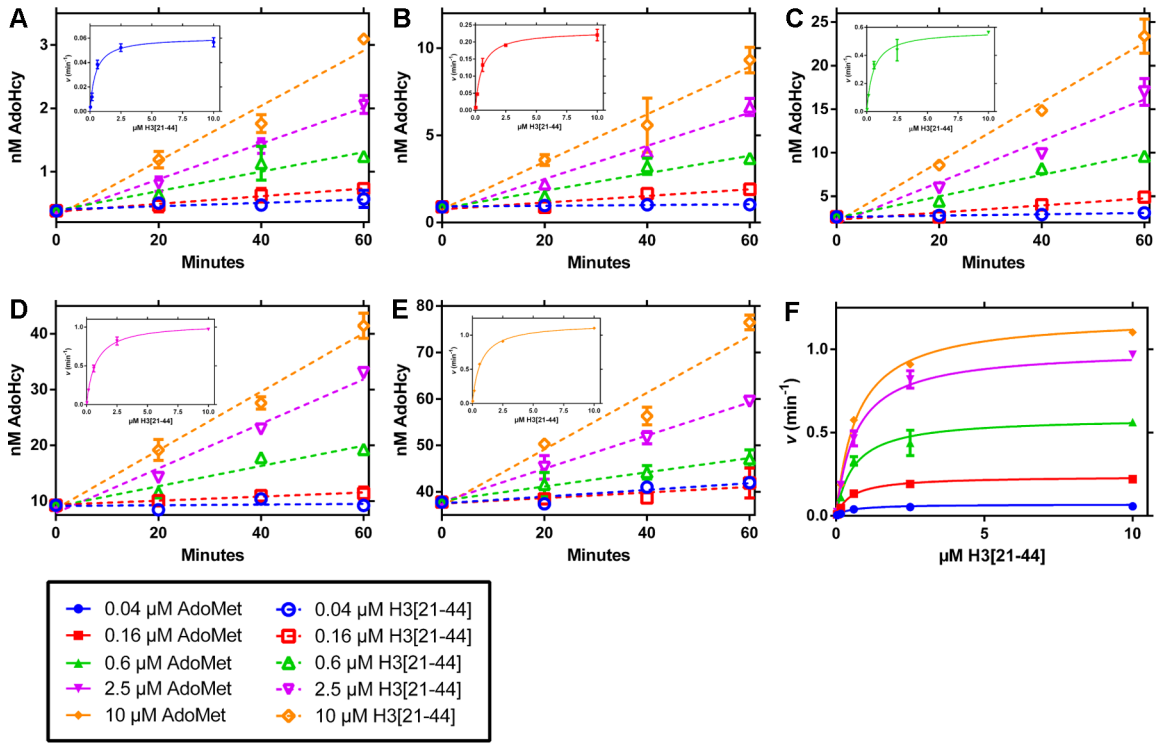

Figure 3. Bisubstrate saturation kinetic analysis of the EZH2 methyltransferase reaction. Graphical representations of the assays performed to obtain catalytic parameters from saturation of both AdoMet and H3[21–44] peptide substrates. The examples represent $PRC2^{WT}$ monomethylation reactions conducted in 20 mM Tris (pH 8.0, ionic strength of 19 mM), 0.5 mM DTT, and 0.01% Triton X-100 at five independent concentrations of H3[21–44] and AdoMet. The slopes of the dotted lines represent initial rates at independent H3[21–44] concentrations from 0.04 to 10 μM in (A) 0.04 μM AdoMet, (B) 0.16 μM AdoMet, (C) 0.6 μM AdoMet, (D) 2.5 μM AdoMet, and (E) 10 μM AdoMet. Insets in panels A–E represent saturation profiles at the corresponding AdoMet concentration, each fit to a single-substrate saturation model (eq 1). (F) Saturation profiles from panels A–E plotted in a single graph, where the solid lines represent the global fits to eq 2.

dx.doi.org/10.1021/bi400805w | *Biochemistry* 2013, 52, 6866–6878

$$\frac{v_n}{v_H} = \sum_i (1 - n - n\Phi_i) \quad (5)$$

where n is the D/H ratio, i is the proton number, and Φ is the proton transition-state fractionation factor (KIE = $1/\Phi$).

RESULTS

Methylation Reaction Specificity. The enzymatic activity of EZH2 relies on specific interactions with at least three members of PRC2; therefore, enzymatic assays must be conducted with purified PRC2 complexes. Accordingly, the experiments described herein were performed using a five-membered complex (including EZH2, SUZ12, RbAp48, AEBP2, and EED), with EZH2 bearing either the WT sequence or the Y641F mutation. The relative enzymatic activity of $PRC2^{WT}$ and $PRC2^{EZH2(Y641F)}$ in mono-, di-, and trimethylation was assessed using a short histone H3 peptide, H3[21−44]. Representative results from these assays are shown in Figure 2, and the catalytic parameters are summarized in Table 1. While $PRC2^{WT}$ is capable of methylating H3[21−44] and H3[21−44(K27-CH_3)] (Figure 2A,B) with catalytic specificity (k_{cat}/K_m) values of (2.28 ± 0.39) and (0.53 ± 0.14) × 10^4 M^{-1} s^{-1}, respectively, no significant activity could accurately be measured on H3{21−44[K27-$(CH_3)_2$]} (Figure 2C). Conversely, $PRC2^{EZH2(Y641F)}$ displayed weak mono- and dimethylation activity, with measured apparent k_{cat}/K_m values of (0.10 ± 0.05) and (0.07 ± 0.03) × 10^4 M^{-1} s^{-1}, respectively, but relatively higher trimethylation activity [k_{cat}/K_m = (1.90 ± 0.20) × 10^4 M^{-1} s^{-1}]. Each reaction with measurable activity gave similar k_{cat} values; however, in the mono- and dimethylation reactions by $PRC2^{EZH2(Y641F)}$, significant substrate inhibition beginning at 30 μM complicated the fit to classical Michaelis−Menten kinetics, resulting in a large error for the reported k_{cat} values in Table 1 (full profiles showing substrate inhibition can be found in Figure S2 of the Supporting Information). Nonetheless, these data are consistent with the observed biological functions of the two complexes and notably the observed increase in the level of trimethylated H3K27 associated with the Y641F mutation.[6,7]

pH−Rate Profiles. To experimentally evaluate the role of general acid−base chemistry in EZH2 catalysis, we measured the pH dependence of initial rates obtained under a variety of conditions. As EZH2 is a bisubstrate enzyme (AdoMet and H3[21−44]), catalytic parameters were obtained by varying the concentration of one substrate at fixed increasing concentrations of the other (Figure 3). Full bisubstrate analysis was performed at each pH unit, and the data were fit globally to eq 2 for a random bi-bi sequential mechanism (Scheme 2) to obtain pH effects on k_{cat}.[40,42]

Notably, the catalytic reaction was shown to be highly sensitive to ionic strength (Figure S1A−C of the Supporting Information); therefore, the salt concentration was kept at the minimal value necessary to maintain consistency at each pH unit (see Experimental Procedures). Additionally, pH stability studies showed irreversible loss of activity beyond pH 9.0 (Figure S1D of the Supporting Information); therefore, saturation kinetic analysis was conducted from pH 7.0 to 9.0 at 0.5 unit increments for $PRC2^{WT}$ mono- and dimethylation (Figures S3 and S4 of the Supporting Information, respectively) and $PRC2^{EZH2(Y641F)}$ trimethylation (Figure S5 of the Supporting Information). pH dependence was assessed by plotting log(k_{cat}) versus pH (Figure 4A,D,G), and pK_a values were obtained by fitting each plot to eq 3 (Table 2).[43] Each methylation reaction showed a basic pH optimum for k_{cat}, with pK_a values for $PRC2^{WT}$ mono- and dimethylation of 7.3 ± 0.1 and 7.7 ± 0.1, respectively, and a pK_a for $PRC2^{EZH2(Y641F)}$ trimethylation of 8.0 ± 0.1. pH−rate profiles for k_{cat}/K_m were measured over multiple substrate concentrations below their K_m values to maximize the accuracy of the data (Figures S6 and S7 of the Supporting Information), and plots of log($k_{cat}/K_{H3[21-44]}$) and log(k_{cat}/K_{AdoMet}) versus pH for each methylation reaction are shown in panels B, E, and H of Figure 4. $k_{cat}/K_{H3[21-44]}$ for each methylation reaction showed basic pH optima, with pK_a values for $PRC2^{WT}$ mono- and dimethylation of 7.7 ± 0.2 and 7.8 ± 0.2, respectively, and a pK_a for $PRC2^{EZH2(Y641F)}$ trimethylation of 7.8 ± 0.2. k_{cat}/K_{AdoMet} profiles, however, were bell-shaped for all three methylation reactions, indicating the independent acidic and basic dependence of interactions between AdoMet and PRC2, and fit to eq 4 to give pK_a values for the acidic optima of 8.9 ± 0.1 for both mono- and dimethylation by $PRC2^{WT}$ and 9.1 ± 0.2 for trimethylation by $PRC2^{EZH2(Y641F)}$. The basic optima measured for k_{cat}/K_{AdoMet} correlate with pK_a values of 7.0 ± 0.1 and 7.4 ± 0.1 for mono- and dimethylation, respectively, by $PRC2^{WT}$ and 7.6 ± 0.2 for trimethylation by $PRC2^{EZH2(Y641F)}$.

Solvent Kinetic Isotope Effects. To explore the possibility of rate-limiting chemistry involving H atoms, we measured catalytic parameters in 90% D_2O compared to normal water solvent [solvent kinetic isotope effects (sKIEs)]. For the EZH2 reaction, deuterium atoms will readily exchange with ζ-hydrogen atoms of lysine, potentially giving primary isotope effects (on bond making or breaking) for any transfers of a proton from lysine at a rate-limiting step. sKIEs on were measured on k_{cat} for $PRC2^{WT}$ mono- and dimethylation and $PRC2^{EZH2(Y641F)}$ trimethylation through full bisubstrate saturation kinetics fit to eq 2. sKIEs on k_{cat} were performed near the pH-independent plateau at pH(D) 9.0 to avoid artifacts due to pH effects from independent buffer preparations and effects of deuterium on buffer pK_a [although these factors were taken into account in preparative steps (see Experimental Procedures)]. Saturation profiles of increasing H3[21−44] peptide concentrations at saturating AdoMet concentrations are illustrated in Figure 5A−C (full bisubstrate profiles are shown in Figure S9 of the Supporting Information). sKIEs are obtained from the ratios of the rates in deuterium to those in protium-based solvent. We measured sKIEs on k_{cat} ($^Dk_{cat}$) for $PRC2^{WT}$ mono- and dimethylation of 1.5 ± 0.1 and 1.8 ± 0.1, respectively, and for $PRC2^{EZH2(Y641F)}$ trimethylation of 1.6 ± 0.1. Next, we measured sKIEs on $k_{cat}/K_{H3[21-44]}$ and k_{cat}/K_{AdoMet} at their respective pH(D)-independent values [pH(D) 9.0 and 8.0, respectively]. For all three methylation reactions, sKIEs were unity [1.0, within experimental error (see Figure S10 and Table S2 of the Supporting Information)].

Proton Inventories. To examine the possibility of multiple protons contributing to the transition state of the methylation reactions catalyzed by $PRC2^{WT}$ and $PRC2^{EZH2(Y641F)}$, we performed proton inventories where the observed sKIE on k_{cat} was measured as a function of the deuterium/protium ratio

Scheme 2. Random Sequential Ternary Bi-Bi Mechanism of Lysine Methylation by EZH2

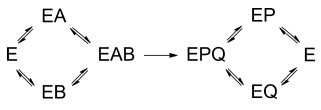

dx.doi.org/10.1021/bi400805w | Biochemistry 2013, 52, 6866−6878

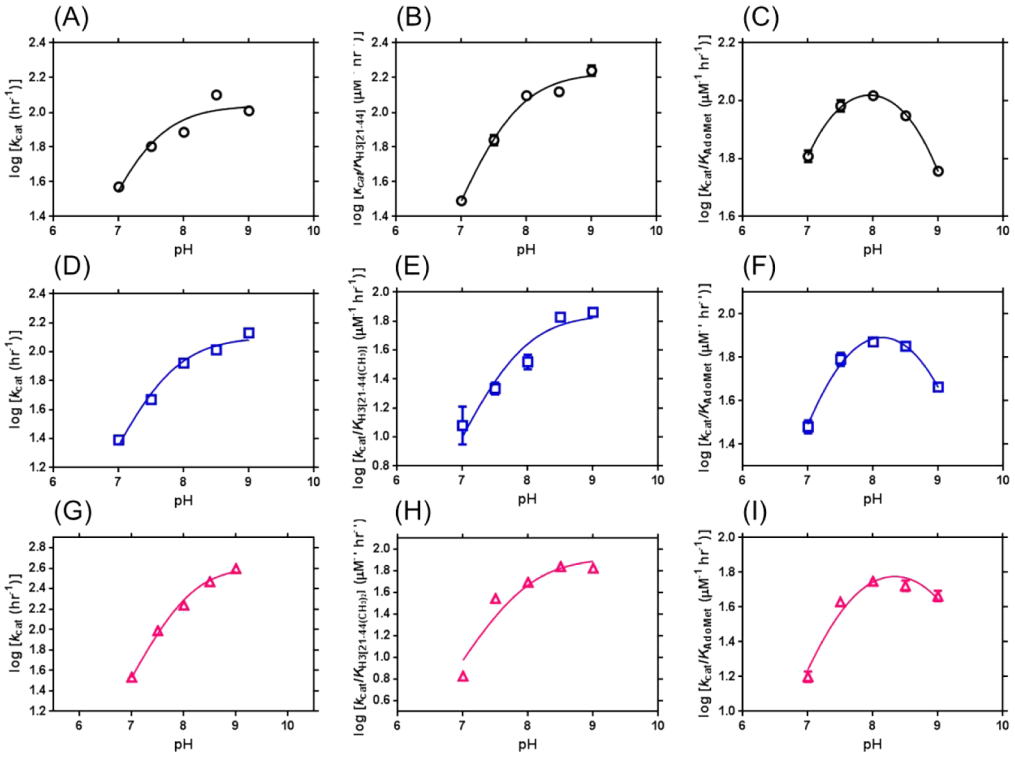

Figure 4. pH−rate profiles for PRC2^{WT} mono- and dimethylation and PRC2$^{EZH2(Y641F)}$ trimethylation. Shown are PRC2^{WT} monomethylation profiles for (A) k_{cat}, (B) $k_{cat}/K_{H3[21-44]}$, and (C) k_{cat}/K_{AdoMet}, PRC2^{WT} dimethylation profiles for (D) k_{cat}, (E) $k_{cat}/K_{H3[21-44(CH3)]}$, and (F) k_{cat}/K_{AdoMet}, and PRC2$^{EZH2(Y641F)}$ trimethylation profiles for (G) k_{cat}, (H) $k_{cat}/K_{H3[21-44(CH_3)_2]}$, and (I) k_{cat}/K_{AdoMet}. Profiles on k_{cat} (A, D, and I) were obtained from full bisubstrate analysis at each pH unit (Figures S3−S5 of the Supporting Information), and profiles on $k_{cat}/K_{H3[21-44]}$ (B, E, and H) and k_{cat}/K_{AdoMet} (C, F, and I) for each reaction were obtained from linear initial rate dependencies at limiting concentrations of each substrate (Figures S6−S8 of the Supporting Information). pK_a values from each profile were obtained by fitting each plot to either eq 3 (for basic plateaus) or eq 4 (for bell-shaped curves), the results of which are summarized in Table 2.

Table 2. pH−Rate Profiles

				k_{cat}/K_{AdoMet} pK_a	
enzyme	peptide substrate	k_{cat} pK_a	$k_{cat}/K_{H3[21-44]}$ pK_a	pK_1	pK_2
PRC2^{WT}	21−44	7.3 ± 0.1	7.7 ± 0.2	7.0 ± 0.1	8.9 ± 0.1
PRC2^{WT}	21−44[K27-CH_3]	7.7 ± 0.1	7.8 ± 0.2	7.4 ± 0.1	8.9 ± 0.1
PRC2$^{EZH2(Y641F)}$	21−44[K27-$(CH_3)_2$]	8.0 ± 0.1	7.8 ± 0.2	7.6 ± 0.2	9.1 ± 0.3

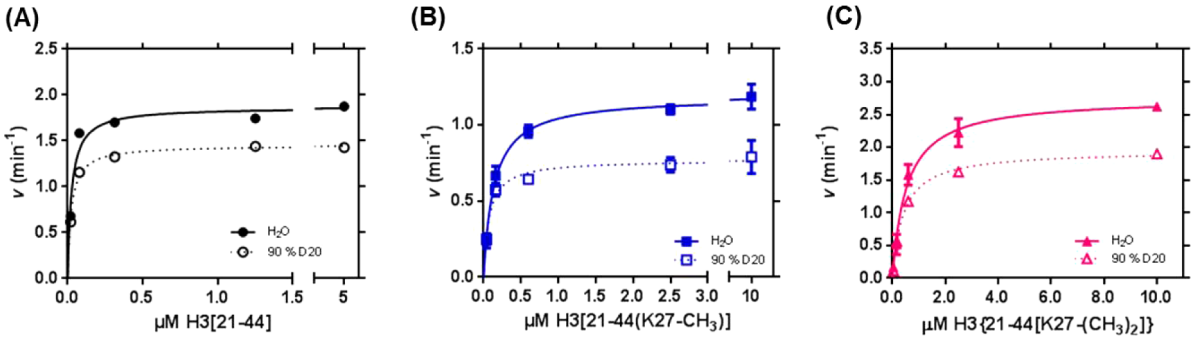

Figure 5. Solvent kinetic isotope effects. Saturation profiles of reactions in H_2O or 90% D_2O solvent with 20 mM Tris [pH(D) 9.0, ionic strength of 6 mM], 0.5 mM DTT, and 0.05% Triton X-100. The graphs are representative curves from 10 μM fixed AdoMet for (A) the PRC2^{WT} monomethylation reaction in H_2O (●, solid line) and 90% D_2O (○, dotted line), (B) PRC2^{WT} dimethylation in H_2O (■, solid line) and 90% D_2O (□, dotted line), and (C) PRC2$^{EZH2(Y641F)}$ trimethylation in H_2O (▲, solid line) and 90% D_2O (△, dotted line). Solvent KIEs on k_{cat} reported were obtained from global fits to the full bisubstrate profiles; however, the plots are shown at 10 μM AdoMet for the sake of simplicity of illustrating the observed isotope effect.

(D/H). Qualitatively, the shape of the resulting curve will be linear (indicating a one-proton transition state) or bowed (indicating a multiproton transition state) because of contributions from each proton.[44] Quantitatively, this curve

dx.doi.org/10.1021/bi400805w | Biochemistry 2013, 52, 6866−6878

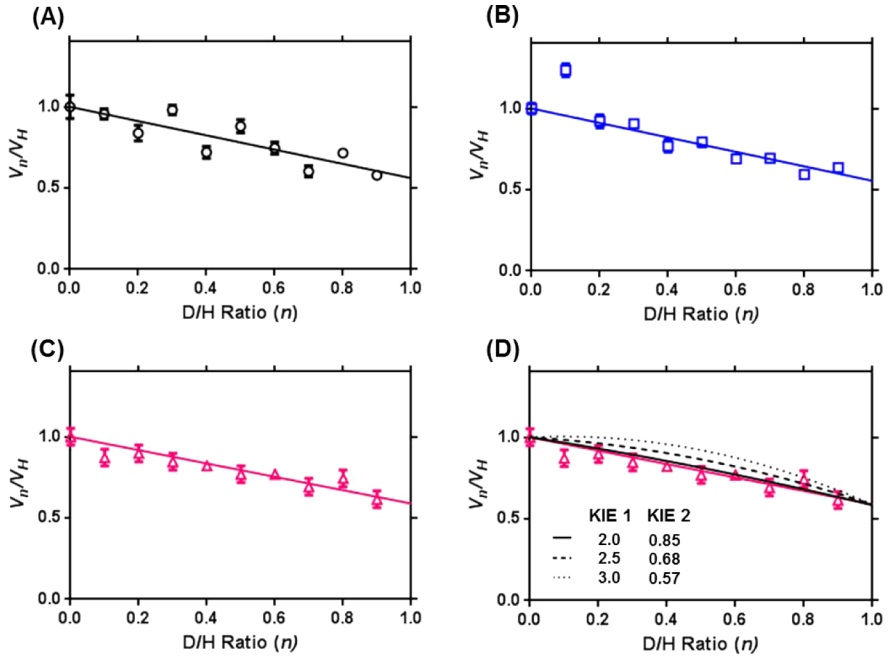

Figure 6. Proton inventories for $PRC2^{WT}$ mono- and dimethylation and $PRC2^{EZH2(Y641F)}$ trimethylation. Ratios of initial rates of reactions in H_2O vs fraction D_2O (V_n/V_H) in 10 μM AdoMet and (A) 10 μM H3[21−44] (monomethylation), (B) 10 μM H3[21−44(K27-CH_3)] (dimethylation), and (C) and 10 μM H3{21−44[K27-$(CH_3)_2$]} (trimethylation) plotted as a function of D/H ratio (n). Solid lines (A−C) represent fits to single-proton transition states (eq 5). (D) Repeat of the trimethylation data shown in panel C with fits to hypothetical two-proton models with substantial inverse and normal contributions from each proton.

Scheme 3. Kinetic Model Consistent with pH−Rate Dependencies

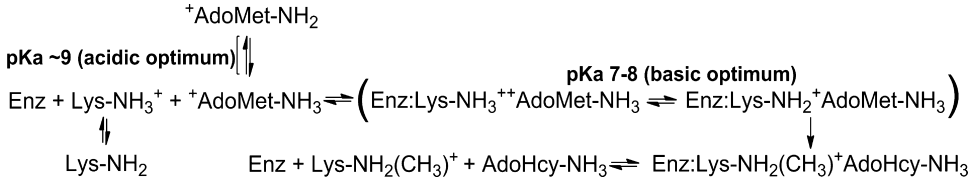

can be fit to eq 5 to obtain transition-state fractionation factors (Φ) for each proton involved in the transition state (Φ values are the inverse of the kinetic isotope effect extrapolated to a D/H ratio of 1.0). Proton inventories for $PRC2^{WT}$ mono- and dimethylation and $PRC2^{EZH2(Y641F)}$ trimethylation are shown in Figure 6A−C. Each curve shows a linear dependency of the isotope effect versus the D/H ratio, with Φ values for single-proton transfers of 0.56 ± 0.03 and 0.55 ± 0.03 for $PRC2^{WT}$ mono- and dimethylation, respectively, and 0.59 ± 0.02 for $PRC2^{EZH2(Y641F)}$ trimethylation.

DISCUSSION

Kinetic analysis of $PRC2^{WT}$ and $PRC2^{EZH2(Y641F)}$ shows that WT EZH2 has significant mono- and dimethylation activity, whereas the Y641F variant favors trimethylation (Figure 2 and Table 1). The similar k_{cat} values for each methylation reaction with measurable activity suggest that the catalytic events that limit steady-state turnover are independent of those that determine substrate and product specificity. The 19- and 27-fold losses of catalytic specificity for mono- and dimethylation, respectively, by $PRC2^{EZH2(Y641F)}$ likely reflect binding or active site interactions that occur before or at the first irreversible step. The observed increase in trimethylation activity upon removal of a hydroxyl group in the Y641F mutant is consistent with a model involving steric hindrance by tyrosine in the lysine binding pocket. However, such a model is incomplete because it cannot account for the observed reduction in the level of mono- and dimethylation in $PRC2^{EZH2(Y641F)}$, which instead suggests an active role of tyrosine in $PRC2^{WT}$. Prior QM/MM studies of SET7/9 showed hydrogen bonding interactions between two hydrogens of Lys-NH_3^+ and the hydroxyl groups of Tyr-245 and Tyr-305, stabilizing the complex for methyl transfer.[32] Independent crystallographic studies of SET7/9 show the same hydrogen bonding behavior for Tyr-245 but instead revealed a water molecule coordinated with Tyr-305 and an ϵ-amino hydrogen atom of lysine.[38] In the WT enzyme, the hydrogen bonds are maintained with methylated lysine and constrain the methyl group in a position that blocks a critical water channel from accessing the active site, preventing subsequent deprotonation and dimethylation. The Y245F mutation (which gives SET7/9 dimethyltransferase activity) supports the methyl group of Lys-$NH_2(CH_3)^+$ in the site previously occupied by the hydroxyl group of tyrosine, permitting water channel access for deprotonation and an additional methyl transfer. As Tyr-245 and Tyr-305 in SET7/9 correspond to Tyr-641 and Ala-697 in EZH2, respectively [by sequence (Figure 1B)], trimethylation may proceed through a similar mechanism in $PRC2^{EZH2(Y641F)}$, consistent with our observation of reduced levels of mono- and dimethylation resulting from a loss of hydrogen bond acceptors for the ϵ-NH_3^+ group of lysine.

dx.doi.org/10.1021/bi400805w | Biochemistry 2013, 52, 6866−6878

The hypothesis that the loss of tyrosine from the lysine binding site reduces the number of hydrogen bonding interactions and supports methyl group occupancy assumes lysine deprotonation occurs on the enzyme and not by bulk solvent when the substrate is free in solution. This was tested with pH−rate profiles under multiple conditions: profiles obtained for second-order rate constants [under conditions of limiting reactant (k_{cat}/K_m)] provide information for any events occurring from reactants free in solution up to and including the first irreversible step in the catalytic cycle, while those obtained for first-order rate constants [where reactants are saturating (k_{cat})] provide information for catalytic events occurring from formation of the ternary complex through release of the products.[42] A schematic model that is supported by the pH−rate data is illustrated in Scheme 3. The observed pH optima on k_{cat} for these reactions (Figure 4 and Table 2) suggest that a specific basic residue within the ternary complex must be deprotonated for the reaction to continue through product release, consistent with enzyme-dependent lysine deprotonation. Similar profiles and pK_a values for $k_{cat}/K_{H3[21-44]}$ and k_{cat} support a model in which the same chemistry is responsible for the observed behavior and together suggest that the requirement for acid/base chemistry occurs after formation of the ternary complex (rule for k_{cat}) and either before or concurrent with the first irreversible step (rule for k_{cat}/K_m). An enzyme-independent deprotonation model in which neutral lysine is the required substrate can likely be ruled out as the pK_a of lysine free in solution is predicted to be ∼10.5 and any reduction of this pK_a to the values measured herein (∼7−8) would be enzyme-dependent (although higher pH optima have been observed in independent PKMT studies,[45] which in those systems may reflect a bypass of the enzyme-dependent deprotonation mechanism with the equilibrium favoring neutral lysine free in solution at the unnaturally high pH values). These conditions, however, could not be tested with PRC2 because of the instability of the complex at pH >9.0 (as previously mentioned). The basic optima shown in the pH−rate profiles for k_{cat}/K_{AdoMet} are also consistent with the $k_{cat}/K_{H3[21-44]}$ and k_{cat} profiles. In contrast, the observed acidic optima are not present in either $k_{cat}/K_{H3[21-44]}$ or k_{cat}, suggesting an effect on AdoMet binding. The pK_a values obtained from the curve fits for k_{cat}/K_{AdoMet} are similar to those predicted for the terminal amine of the methionine moiety of AdoMet (∼9.0), which may suggest preferential binding of protonated methionine in the AdoMet binding pocket.

Three mechanistic models have stemmed from a variety of studies that address enzymatic lysine deprotonation by PKMTs, one suggesting an essential tyrosine (Y726 in EZH2) acts as a general base, another suggesting preferential binding to Lys-ε-NH_2, and the other suggesting a ternary complex-induced water channel gives active site access to bulk solvent. Our pH−-rate data are sufficient to rule out enzyme-independent solvent deprotonation of lysine prior to binding. However, qualitatively, our pH−rate data are insufficient to rule out either on-enzyme mechanism, as we can support only a model of enzyme-dependent acid/base chemistry. However, computational models of the ternary complex of SET7/9 in monomethylation gave calculated pK_a values of 8.2 ± 0.6 for lysine and 16.6 ± 4.2 for the essential tyrosine.[32] A comparison of our experimental pK_a values with these theoretical values shows good agreement with the calculated value for lysine, supporting enzyme-dependent equilibrium dissociation of the proton into bulk solvent in EZH2. Furthermore, amine methylation is consistent with an increase in its pK_a, providing additional support for dissociation of the lysine proton to water from H3[21−44], H3[21−44(K27-CH_3)], and H3{21−44[(K27-$CH_3)_2$]} substrates, which in these experiments gave k_{cat} pK_a values of 7.3, 7.7, and 8.0, respectively.

Although our data better support enzyme-dependent solvent deprotonation of lysine, it is important to point out that the proposed tyrosine that has been suggested to act as a general base (Y726 in EZH2) is absolutely conserved in SET domain PKMTs and is essential for catalytic activity. Structural and kinetic analyses performed on *v*SET (a viral H3K27 methyltransferase) generated a hypothesis that held that the essential tyrosine participates in the proper alignment of an enzymatic lysine access channel.[46] Additional studies have suggested that the essential tyrosine provides structural stability by participating in critical hydrogen bonding with the enzyme main chain,[24] while another has suggested the hydroxyl of the corresponding tyrosine in SET7/9, Y335, participates in hydrogen bonding with the methyl hydrogen atoms of AdoMet.[47] Therefore, there are many possible roles for the essential tyrosine residue that do not necessarily involve its participation as a general base.

Enzymatic lysine deprotonation suggests that the proton transfer may occur as part of a rate-limiting (or partially rate-limiting) step in the catalytic cycle. We tested this by measuring solvent kinetic isotope effects. Heavy isotope substitution changes bond vibrational frequency, and isotope effects report on differences in the bonding environment between two states. A sKIE is observed when the bonding environment of the labeled atom is changed in a rate-determining step relative to the ground state. In enzymatic reactions, these can be (1) binding effects, (2) intermediate equilibrium effects, (3) chemical transformation (transition-state) effects (intrinsic KIEs), or (4) product equilibrium effects.[48] Interpretation of KIEs follows the same rules on k_{cat}/K_m and k_{cat} as pH−rate profiles. However, instead of reporting on acid/base chemistry, isotope effects on k_{cat}/K_m and k_{cat} report on a changed bonding environment at the step limiting the observed rate. The observed sKIEs on k_{cat} are consistent with a change in the bonding environment for hydrogen at a rate-limiting step, supporting lysine deprotonation as being partially rate-limiting. These values were the same within experimental error for the $PRC2^{WT}$ mono- and dimethylation and $PRC2^{EZH2(Y641F)}$ trimethylation reactions, suggesting the chemical mechanism of lysine deprotonation is the same for each reaction. Furthermore, the $PRC2^{EZH2(Y641F)}$ reaction uses H3{21−44[K27-$(CH_3)_2$]} as a substrate, which unlike the mono- and dimethylation substrates has only one ζ-hydrogen atom to exchange with solvent. Therefore, if the observed sKIE reports on the transition state of lysine deprotonation, the effect must be primary for at least the trimethylation reaction, as no ζ-deuterium atoms are present to give a secondary isotope effect.

The absence of a measurable sKIE, within experimental error, on k_{cat}/K_{AdoMet} or $k_{cat}/K_{H3[21-44]}$ parameters for each methylation reaction can indicate that (1) the KIE-sensitive step for k_{cat} occurs after the first irreversible step, (2) an inverse binding or intermediate equilibrium isotope effect offsets the k_{cat} KIE, or (3) the KIEs on k_{cat}/K_{AdoMet} and $k_{cat}/K_{H3[21-44]}$ are suppressed by forward commitment factors (probability of bound substrate proceeding toward product vs dissociating from the ternary complex[48]). In the first possible scenario, the pH-dependent step must be different for k_{cat} and for k_{cat}/K_{AdoMet} and $k_{cat}/K_{H3[21-44]}$; otherwise, the observed KIE might

dx.doi.org/10.1021/bi400805w | *Biochemistry* 2013, 52, 6866−6878

Scheme 4. Chemical Mechanism from pH−Rate Profiles and Solvent KIEs

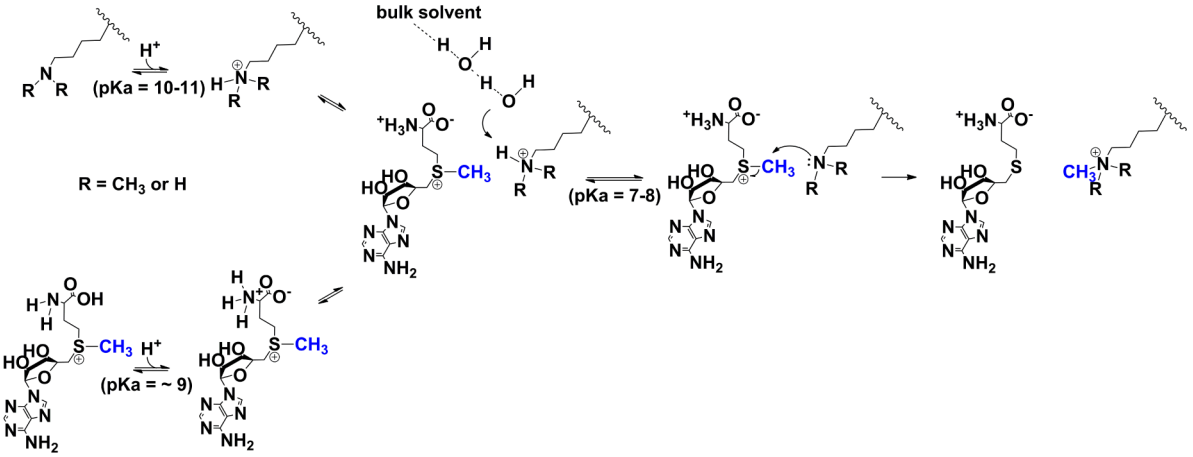

be expected to be comparable for each parameter. In the second possible scenario, pH−rate profiles for k_{cat} and $k_{cat}/K_{H3[21-44]}$ may reflect the deprotonation of lysine, with the normal $^{D}k_{cat}$ reporting on partially rate-limiting deprotonation chemistry and an inverse $^{D}(k_{cat}/K_{H3[21-44]})$ and $^{D}(k_{cat}/K_{AdoMet})$ equilibrium isotope effect upon ternary complex formation that offsets the normal KIE resulting from deprotonation chemistry. Alternatively, k_{cat}/K_{AdoMet} and $k_{cat}/K_{H3[21-44]}$ profiles could reflect lysine deprotonation chemistry, and k_{cat} could reflect a second proton transfer, either at a partially rate-limiting step offsetting the KIE on k_{cat}/K_{AdoMet} and $k_{cat}/K_{H3[21-44]}$ or after the first irreversible step (presumably methyl transfer). In this multiple-proton mechanism, the pH-dependent behavior of k_{cat} would likely reflect a basic amino acid within the enzyme with a pK_a nearly identical to that of the group(s) responsible for the observed pH−rate profiles on k_{cat}/K_{AdoMet} and $k_{cat}/K_{H3[21-44]}$. In the third possible scenario, external forward commitment factors could suppress the observed KIE on k_{cat}/K_{AdoMet} and $k_{cat}/K_{H3[21-44]}$. Accordingly, significant forward commitment factors might also be expected to influence the pH−rate dependence of k_{cat}/K_{AdoMet} and $k_{cat}/K_{H3[21-44]}$ through a reduced apparent pK_a value. However, the influence of the forward commitment on the pH−rate profiles described herein can be masked by additional factors unrelated to the commitment[42] (see Supplementary Discussion in the Supporting Information). Given the relatively small magnitude of the observed sKIEs on k_{cat}, commitment factors sufficient to suppress the sKIE values near unity, within error, may not be reflected in the pK_a values, as the shifts in pK_a may fall within the error of the measurement. Therefore, it is possible that a suppression of the observed KIE on k_{cat}/K_{AdoMet} and $k_{cat}/K_{H3[21-44]}$ could be due to forward commitment factors that would not necessarily be reflected in the pH−rate profiles. As the pH−rate profiles indicate similar basic optima for k_{cat}, $k_{cat}/K_{H3[21-44]}$, and k_{cat}/K_{AdoMet}, we postulate that they report on the same chemical step and that suppressed KIEs may be attributed to commitment factors.

The solvent KIEs measured on k_{cat} suggest lysine deprotonation occurs at a partially rate-limiting step in the EZH2 methyltransferase reaction. We used proton inventories to explore the possibility of multiple protons contributing to the observed sKIE. Although our data best fit to a single-proton model, it is important to note that the small magnitude of the observed KIE reduces the distinction between a single proton and small contributions from multiple protons. We can, however, rule out the possibility of substantially large normal (KIE > 1.0) and inverse (KIE < 1.0) effects combining to give the observed KIE, the result of which could be a significant and visible bowing effect (Figure 5D). Furthermore, the proton inventory data provide additional support for a proton transfer occurring during a partially rate-limiting step in the catalytic cycle.

Previous computational studies have suggested the highest energy barrier for EZH2 catalysis is at a 50% dissociative transition state for methyl transfer, with no energy barrier at the QM/MM level for the transfer of a hydrogen from Lys-ε-NH_3^+ to $^-$OH when treated as an independent step.[36] In contrast, our data suggest lysine deprotonation is at least partially rate-limiting; therefore, a mechanism involving concerted lysine deprotonation and methyl transfer seems logical energetically. However, observations of the reversibility of deprotonation (defined by its pK_a) and the irreversibility of methyl transfer are inconsistent with this model. As the solvent deprotonation is suggested to be enzyme-dependent, a possible interpretation is that enzymatic events (such as protein motions involved in opening of the water channel) associated with the deprotonation equilibrium contribute to the rate limitation of the reaction in such a way that an equilibrium between solvent and lysine can only occur at an energy state of the enzyme that is sufficiently high to limit the rate of the reaction. In this model, the solvent KIE would report on the transfer of the proton to solvent to form this higher-energy intermediate, which subsequently proceeds to methyl transfer.

A chemical mechanism that is consistent with our pH−rate profiles and solvent kinetic isotope effects is illustrated in Scheme 4. Within the pH range permitted by EZH2 stability, our data suggest that both AdoMet and H3K27 bind to the enzyme with the terminal NH_3^+ of the methionine moiety of AdoMet and the ε-NH_3^+ of the methyl-accepting lysine in their acidic forms. Formation of the ternary complex then permits access of the enzyme active site to bulk solvent, which then deprotonates lysine because of its reduced pK_a resulting from the charge−charge interaction with the S^+-CH_3 of AdoMet. Following deprotonation, the methyl group is transferred from AdoMet to ε-NH_2-Lys in an assumed S_N2 substitution reaction.

The existence of a water channel in EZH2 to allow for lysine deprotonation is speculative, as there remains no supporting crystallographic evidence to date. However, the water channel hypothesis has been suggested for alternative SET domain PKMTs,[31−36] and sequence similarities and functional con-

dx.doi.org/10.1021/bi400805w | Biochemistry 2013, 52, 6866−6878

sequences of key mutations in analogous residues in EZH2 suggest that the active form of the enzyme has a similar structure. Additionally, there have been reports of SET domain PKMTs proceeding processively[45] (the substrate lysine is not released by the enzyme prior to the next round of deprotonation and methyl transfer). This suggests that at some point in the reaction cycle, water must access the active site, whether to deprotonate lysine itself or to deprotonate a general base to allow for an additional round of chemistry. Although EZH2 does not follow a processive mechanism in our biochemical assays, we cannot rule out the possibility under native conditions. Furthermore, the similarity in sequence and essential residues across SET domain PKMTs suggests that the mechanism is conserved and that although some PKMTs may not require processivity for regulatory purposes, the ability to accommodate such a mechanism may be retained.

Tyrosine residues in the lysine binding site in a variety of SET domain PKMTs have been shown to correlate with mono-, di-, or trimethylation specificity. Indeed, the EZH2 Y641F mutant studied here showed significantly higher activity in trimethylation and reduced activity if mono- and dimethylation compared to that of WT EZH2. This is consistent with a model in which tyrosine residues provide stabilizing hydrogen bonds to ε-NH_3^+-Lys but can also prevent subsequent methylation rounds by holding the methyl group in a position that blocks solvent access for another round of methylation. The resulting loss of these hydrogen bonds in the Y641F mutant of EZH2 correlates with the observed loss-of-function behavior of $PRC2^{EZH2(Y641F)}$ in mono- and dimethylation. This is also consistent with the observed gain-of-function behavior in trimethylation resulting from the loss of a hydrogen bond with ε-$NH(CH_3)_2^+$-Lys, which permits its deprotonation.

CONCLUSIONS

EZH2, the catalytic subunit of PRC2, methylates lysine 27 of histone 3. While EZH2 has mono- and dimethylation activity, the Y641F variant favors trimethylation. Our pH−rate analyses revealed basic pH profiles for k_{cat} and $k_{cat}/K_{H3[21-44]}$ and bell-shaped profiles for k_{cat}/K_{AdoMet} for each methylation reaction, the values of which support an enzyme-dependent lysine deprotonation model. The pK_a values obtained from the pH−rate studies correlate with calculated pK_a values from a previously proposed computational model in which the ternary Lys-ε-NH_3^+·AdoMet·Enz complex induces formation of a water channel that permits solvent access to deprotonate lysine.[32] Solvent kinetic isotope effect analyses suggest a change in the ζ-hydrogen bonding environment of lysine in a rate-limiting step of the EZH2 catalytic cycle, consistent with lysine deprotonation being at least partially rate-limiting.

The role of EZH2 in multiple cancers suggests a high potential therapeutic value for EZH2 inhibitors. Experimental studies of the chemical details of enzymatic mechanisms, such as those described here for EZH2, can provide valuable tools for the strategic design of specific inhibitors with potential clinical use. Although it is widely assumed that PKMTs proceed through an S_N2 mechanism, critical details of active site chemistry (such as charge distribution throughout the reaction) can substantially influence the binding properties of potential inhibitors. In the PKMT reaction, the electrostatic environment of the active site upon binding of both positively charged AdoMet and ε-NH_3^+-lysine differs significantly from that of the AdoMet·ε-NH_2-lysine intermediate. During methyl transfer, the charge moves from the AdoMet binding site, through the SET domain "tunnel", to the ε-NH_2 moiety of the lysine substrate to give ε-$NH_2(CH_3)^+$. The positive electrostatic distribution at the transition state of methyl transfer has not yet been explored; however, such information could provide a powerful basis for future transition-state analogue drug design. As our observations described here suggest that the enzymatic deprotonation of lysine occurs in a manner independent of methyl transfer and also occurs at a rate-limiting step, there are independent transition-state barriers that could serve as a potential basis for transition-state analogue inhibitor design for EZH2.

ASSOCIATED CONTENT

Supporting Information

Ionic strength, pH stability, mono- and dimethylation substrate inhibition of $PRC2^{EZH2(Y641F)}$, bisubstrate saturation plots and analyses for pH−rate and solvent KIE studies, k_{cat}/K_{AdoMet} and $k_{cat}/K_{H3[21-44]}$ pH−rate plots and analyses, and Supplementary Discussion of the forward commitment to catalysis. This material is available free of charge via the Internet at http://pubs.acs.org.

AUTHOR INFORMATION

Corresponding Author

*Novartis Institutes for Biomedical Research (NIBR), 250 Massachusetts Ave., Cambridge, MA 02139. E-mail: pascal.fortin@novartis.com. Telephone: (617) 871-3458.

Funding

This work was supported in part by NIBR Education, Diversity, & Inclusion through the Presidential Postdoctoral Fellowship program and by Oncology, NIBR.

Notes

The authors declare no competing financial interest.

ACKNOWLEDGMENTS

We thank Daniel A. King (Center for Proteomic Chemistry, NIBR) for providing PRC2 protein. We also thank William R. Sellers, Yanqiu Yuan, and Peter W. White (Oncology, NIBR) for their critical reading of the manuscript.

REFERENCES

(1) Bonasio, R., Tu, S., and Reinberg, D. (2010) Molecular signals of epigenetic states. *Science 330* (6004), 612−616.

(2) Egger, G., Liang, G., Aparicio, A., and Jones, P. A. (2004) Epigenetics in human disease and prospects for epigenetic therapy. *Nature 429* (6990), 457−463.

(3) Andreoli, F., Barbosa, A. J., Parenti, M. D., and Del, R. A. (2013) Modulation of epigenetic targets for anticancer therapy: Clinicopathological relevance, structural data and drug discovery perspectives. *Curr. Pharm. Des. 19* (4), 578−613.

(4) Nimura, K., Ura, K., and Kaneda, Y. (2010) Histone methyltransferases: Regulation of transcription and contribution to human disease. *J. Mol. Med. (Heidelberg, Ger.) 88* (12), 1213−1220.

(5) Copeland, R. A., Solomon, M. E., and Richon, V. M. (2009) Protein methyltransferases as a target class for drug discovery. *Nat. Rev. Drug Discovery 8* (9), 724−732.

(6) Chang, C. J., and Hung, M. C. (2012) The role of EZH2 in tumour progression. *Br. J. Cancer 106* (2), 243−247.

(7) Yap, D. B., Chu, J., Berg, T., Schapira, M., Cheng, S. W., Moradian, A., Morin, R. D., Mungall, A. J., Meissner, B., Boyle, M., Marquez, V. E., Marra, M. A., Gascoyne, R. D., Humphries, R. K., Arrowsmith, C. H., Morin, G. B., and Aparicio, S. A. (2011) Somatic mutations at EZH2 Y641 act dominantly through a mechanism of selectively altered PRC2 catalytic activity, to increase H3K27 trimethylation. *Blood 117* (8), 2451−2459.

(8) Sneeringer, C. J., Scott, M. P., Kuntz, K. W., Knutson, S. K., Pollock, R. M., Richon, V. M., and Copeland, R. A. (2010) Coordinated activities of wild-type plus mutant EZH2 drive tumor-associated hypertrimethylation of lysine 27 on histone H3 (H3K27) in human B-cell lymphomas. *Proc. Natl. Acad. Sci. U.S.A. 107* (49), 20980−20985.
(9) McCabe, M. T., Ott, H. M., Ganji, G., Korenchuk, S., Thompson, C., Van Aller, G. S., Liu, Y., Graves, A. P., Della, P. A., III, Diaz, E., LaFrance, L. V., Mellinger, M., Duquenne, C., Tian, X., Kruger, R. G., McHugh, C. F., Brandt, M., Miller, W. H., Dhanak, D., Verma, S. K., Tummino, P. J., and Creasy, C. L. (2012) EZH2 inhibition as a therapeutic strategy for lymphoma with EZH2-activating mutations. *Nature 492* (7427), 108−112.
(10) Chase, A., and Cross, N. C. (2011) Aberrations of EZH2 in cancer. *Clin. Cancer Res. 17* (9), 2613−2618.
(11) Karanikolas, B. D., Figueiredo, M. L., and Wu, L. (2009) Polycomb group protein enhancer of zeste 2 is an oncogene that promotes the neoplastic transformation of a benign prostatic epithelial cell line. *Mol. Cancer Res. 7* (9), 1456−1465.
(12) Crea, F., Hurt, E. M., Mathews, L. A., Cabarcas, S. M., Sun, L., Marquez, V. E., Danesi, R., and Farrar, W. L. (2011) Pharmacologic disruption of Polycomb Repressive Complex 2 inhibits tumorigenicity and tumor progression in prostate cancer. *Mol. Cancer 10*, 40.
(13) Gonzalez, M. E., Li, X., Toy, K., DuPrie, M., Ventura, A. C., Banerjee, M., Ljungman, M., Merajver, S. D., and Kleer, C. G. (2009) Downregulation of EZH2 decreases growth of estrogen receptor-negative invasive breast carcinoma and requires BRCA1. *Oncogene 28* (6), 843−853.
(14) Puppe, J., Drost, R., Liu, X., Joosse, S. A., Evers, B., Cornelissen-Steijger, P., Nederlof, P., Yu, Q., Jonkers, J., van, L. M., and Pietersen, A. M. (2009) BRCA1-deficient mammary tumor cells are dependent on EZH2 expression and sensitive to Polycomb Repressive Complex 2-inhibitor 3-deazaneplanocin A. *Breast Cancer Res. 11* (4), R63.
(15) Cao, R., Wang, L., Wang, H., Xia, L., Erdjument-Bromage, H., Tempst, P., Jones, R. S., and Zhang, Y. (2002) Role of histone H3 lysine 27 methylation in Polycomb-group silencing. *Science 298* (5595), 1039−1043.
(16) Schapira, M. (2011) Structural Chemistry of Human SET Domain Protein Methyltransferases. *Curr. Chem. Genomics 5* (Suppl. 1), 85−94.
(17) Del Rizzo, P. A., and Trievel, R. C. (2011) Substrate and product specificities of SET domain methyltransferases. *Epigenetics 6* (9), 1059−1067.
(18) Dillon, S. C., Zhang, X., Trievel, R. C., and Cheng, X. (2005) The SET-domain protein superfamily: Protein lysine methyltransferases. *Genome Biol. 6* (8), 227.
(19) Cheng, X., Collins, R. E., and Zhang, X. (2005) Structural and sequence motifs of protein (histone) methylation enzymes. *Annu. Rev. Biophys. Biomol. Struct. 34*, 267−294.
(20) Copeland, R. A., Moyer, M. P., and Richon, V. M. (2013) Targeting genetic alterations in protein methyltransferases for personalized cancer therapeutics. *Oncogene 32* (8), 939−946.
(21) Cosgrove, M. S., and Patel, A. (2010) Mixed lineage leukemia: A structure-function perspective of the MLL1 protein. *FEBS J. 277* (8), 1832−1842.
(22) Couture, J. F., Collazo, E., Brunzelle, J. S., and Trievel, R. C. (2005) Structural and functional analysis of SET8, a histone H4 Lys-20 methyltransferase. *Genes Dev. 19* (12), 1455−1465.
(23) McCabe, M. T., Graves, A. P., Ganji, G., Diaz, E., Halsey, W. S., Jiang, Y., Smitheman, K. N., Ott, H. M., Pappalardi, M. B., Allen, K. E., Chen, S. B., Della, P. A., III, Dul, E., Hughes, A. M., Gilbert, S. A., Thrall, S. H., Tummino, P. J., Kruger, R. G., Brandt, M., Schwartz, B., and Creasy, C. L. (2012) Mutation of A677 in histone methyltransferase EZH2 in human B-cell lymphoma promotes hypertrimethylation of histone H3 on lysine 27 (H3K27). *Proc. Natl. Acad. Sci. U.S.A. 109* (8), 2989−2994.
(24) Xiao, B., Jing, C., Wilson, J. R., Walker, P. A., Vasisht, N., Kelly, G., Howell, S., Taylor, I. A., Blackburn, G. M., and Gamblin, S. J. (2003) Structure and catalytic mechanism of the human histone methyltransferase SET7/9. *Nature 421* (6923), 652−656.
(25) Zhang, X., Yang, Z., Khan, S. I., Horton, J. R., Tamaru, H., Selker, E. U., and Cheng, X. (2003) Structural basis for the product specificity of histone lysine methyltransferases. *Mol. Cell 12* (1), 177−185.
(26) Trievel, R. C., Beach, B. M., Dirk, L. M., Houtz, R. L., and Hurley, J. H. (2002) Structure and catalytic mechanism of a SET domain protein methyltransferase. *Cell 111* (1), 91−103.
(27) Kwon, T., Chang, J. H., Kwak, E., Lee, C. W., Joachimiak, A., Kim, Y. C., Lee, J., and Cho, Y. (2003) Mechanism of histone lysine methyl transfer revealed by the structure of SET7/9-AdoMet. *EMBO J. 22* (2), 292−303.
(28) Wu, H., Min, J., Lunin, V. V., Antoshenko, T., Dombrovski, L., Zeng, H., Allali-Hassani, A., Campagna-Slater, V., Vedadi, M., Arrowsmith, C. H., Plotnikov, A. N., and Schapira, M. (2010) Structural biology of human H3K9 methyltransferases. *PLoS One 5* (1), e8570.
(29) Guo, H. B., and Guo, H. (2007) Mechanism of histone methylation catalyzed by protein lysine methyltransferase SET7/9 and origin of product specificity. *Proc. Natl. Acad. Sci. U.S.A. 104* (21), 8797−8802.
(30) Trievel, R. C., Flynn, E. M., Houtz, R. L., and Hurley, J. H. (2003) Mechanism of multiple lysine methylation by the SET domain enzyme Rubisco LSMT. *Nat. Struct. Biol. 10* (7), 545−552.
(31) Zhang, X., and Bruice, T. C. (2008) Product specificity and mechanism of protein lysine methyltransferases: Insights from the histone lysine methyltransferase SET8. *Biochemistry 47* (25), 6671−6677.
(32) Zhang, X., and Bruice, T. C. (2008) Enzymatic mechanism and product specificity of SET-domain protein lysine methyltransferases. *Proc. Natl. Acad. Sci. U.S.A. 105* (15), 5728−5732.
(33) Zhang, X., and Bruice, T. C. (2008) Mechanism of product specificity of AdoMet methylation catalyzed by lysine methyltransferases: Transcriptional factor p53 methylation by histone lysine methyltransferase SET7/9. *Biochemistry 47* (9), 2743−2748.
(34) Zhang, X., and Bruice, T. C. (2007) Histone lysine methyltransferase SET7/9: Formation of a water channel precedes each methyl transfer. *Biochemistry 46* (51), 14838−14844.
(35) Zhang, X., and Bruice, T. C. (2007) A quantum mechanics/molecular mechanics study of the catalytic mechanism and product specificity of viral histone lysine methyltransferase. *Biochemistry 46* (34), 9743−9751.
(36) Zhang, X., and Bruice, T. C. (2007) Catalytic mechanism and product specificity of rubisco large subunit methyltransferase: QM/MM and MD investigations. *Biochemistry 46* (18), 5505−5514.
(37) Couture, J. F., Dirk, L. M., Brunzelle, J. S., Houtz, R. L., and Trievel, R. C. (2008) Structural origins for the product specificity of SET domain protein methyltransferases. *Proc. Natl. Acad. Sci. U.S.A. 105* (52), 20659−20664.
(38) Del Rizzo, P. A., Couture, J. F., Dirk, L. M., Strunk, B. S., Roiko, M. S., Brunzelle, J. S., Houtz, R. L., and Trievel, R. C. (2010) SET7/9 catalytic mutants reveal the role of active site water molecules in lysine multiple methylation. *J. Biol. Chem. 285* (41), 31849−31858.
(39) Qi, W., Chan, H. M., Teng, L., Li, L., Chuai, S. N., Zhang, R. P., Zeng, J., Li, M., Fan, H., Lin, Y., Gu, J., Ardayfio, O., Zhang, J. H., Yan, X. X., Fang, J. L., Mi, Y., Zhang, M., Zhou, T., Feng, G., Chen, Z. J., Li, G. B., Yang, T., Zhao, K. H., Liu, X. H., Yu, Z. T., Lu, C. X., Atadja, P., and Li, E. (2012) Selective inhibition of Ezh2 by a small molecule inhibitor blocks tumor cells proliferation. *Proc. Natl. Acad. Sci. U.S.A. 109* (52), 21360−21365.
(40) Swalm, B. M., Hallenbeck, K. K., Majer, C. R., Jin, L., Scott, M. P., Moyer, M. P., Copeland, R. A., and Wigle, T. J. (2013) Convergent evolution of chromatin modification by structurally distinct enzymes: comparative enzymology of histone H3 Lys27 methylation by human polycomb repressive complex 2 and vSET. *Biochem. J. 453* (2), 241−247.
(41) Stein, R. L. (2011) *Kinetics of Enzyme Action*, John Wiley & Sons, Inc., Hoboken, NJ.

(42) Cook, P. F., and Cleland, W. W. (2007) *Enzyme Kinetics and Mechanism*, Garland Science Publishing, New York.
(43) Hyland, L. J., Tomaszek, T. A., Jr., and Meek, T. D. (1991) Human immunodeficiency virus-1 protease. 2. Use of pH rate studies and solvent kinetic isotope effects to elucidate details of chemical mechanism. *Biochemistry 30* (34), 8454−8463.
(44) Venkatasubban, K. S., and Schowen, R. L. (1984) The proton inventory technique. *CRC Crit. Rev. Biochem. 17* (1), 1−44.
(45) Dirk, L. M., Flynn, E. M., Dietzel, K., Couture, J. F., Trievel, R. C., and Houtz, R. L. (2007) Kinetic manifestation of processivity during multiple methylations catalyzed by SET domain protein methyltransferases. *Biochemistry 46* (12), 3905−3915.
(46) Qian, C., Wang, X., Manzur, K., Sachchidanand, Farooq, A., Zeng, L., Wang, R., and Zhou, M. M. (2006) Structural insights of the specificity and catalysis of a viral histone H3 lysine 27 methyltransferase. *J. Mol. Biol. 359* (1), 86−96.
(47) Horowitz, S., Yesselman, J. D., Al-Hashimi, H. M., and Trievel, R. C. (2011) Direct evidence for methyl group coordination by carbon-oxygen hydrogen bonds in the lysine methyltransferase SET7/9. *J. Biol. Chem. 286* (21), 18658−18663.
(48) Cleland, W. W. (2005) The use of isotope effects to determine enzyme mechanisms. *Arch. Biochem. Biophys. 433* (1), 2−12.